Chapter 1. Introduction

Statement of the Problem.

The goal of this research is to develop and study a supramolecular system coupling two light absorbers to a central metal capable of collecting two electrons. In a previous device for photoinitiated electron collection developed by Brewer and co-workers, $\{[(bpy)_2Ru(dpb)]_2IrCl_2\}(PF_6)_5$, electron collection was delocalized over a larger $(dpb)Ir^{III}(dpb)$ portion of the molecule. The complex under investigation in this thesis is $\{[(bpy)_2Ru(dpp)]_2RhCl_2\}(PF_6)_5$, where bpy = 2,2'-bipyridine, and dpp = 2,3-bis(2-pyridyl)pyrazine. The central metal (Rh) and bridging ligands (dpp) tune the energy levels such that electron collection on the central Rh is favored. Cyclic voltammetry and bulk electrolysis studies are used to investigate the properties of the complex upon two-electron reduction of the $Rh(dpp)_2Cl_2$ moiety.

Review of the Related Literature.

Molecular Orbital Representation of Octahedral Complexes.

The spectroscopic and electrochemical properties of transition metal complexes are typically described using molecular orbitals. For pseudo octahedral d^6 metal complexes, like Ru(II) polypyridyl complexes, the molecular orbital picture is commonly described by the linear combination of atomic orbitals (LCAO) theory (Figure 1.1). Figure 1.1 depicts a molecular orbital diagram for an octahedral complex with both σ bonding and π back-bonding. The s, p, and d metal orbitals combine with the σ, π, and/or δ ligand orbitals to form molecular orbitals. The highest occupied molecular orbital (HOMO) for the metal complex is primarily metal-based ($d\pi$) in character. The lowest unoccupied molecular orbital (LUMO) for the metal complex is often primarily ligand-based (π^*) in character. There can be cases where the t_{2g}^* (π^*_L) set is lower in energy that the e_g^* (σ^*_M) set (and reverse) depending on the degree of interaction (both π and σ). These frontier orbitals play a key role in photochemical and redox processes.[1] The HOMO will be the orbital involved in oxidation, the LUMO in reduction.

Figure 1.1. Block Molecular Orbital Representation of Octahedral Ru(II) Complexes.[1]

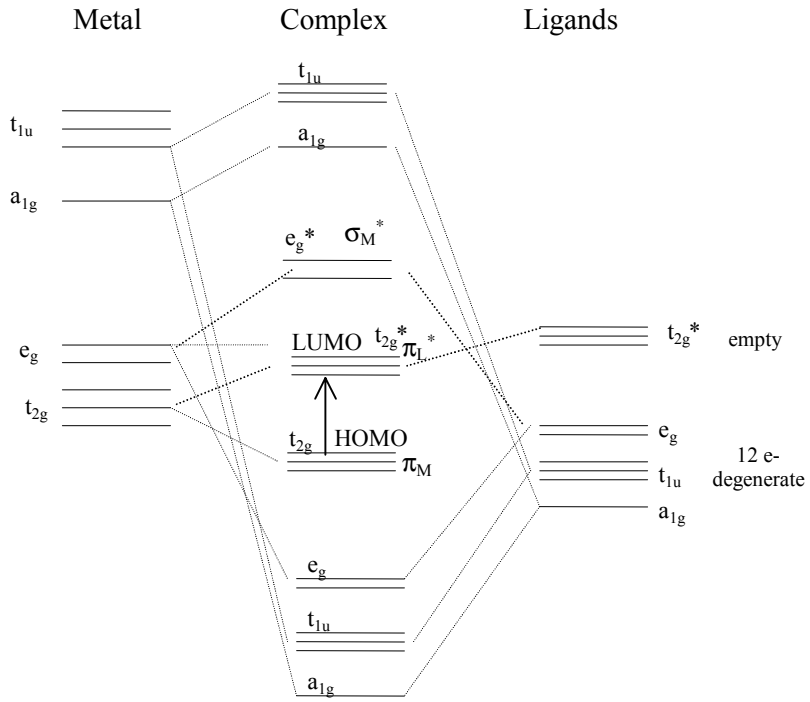

MLCT is represented by an arrow.

Ruthenium Polypyridyl Complexes.

In 1936, F. H. Burnstall published the first synthesis and characterization of $[Ru(bpy)_3]^{+2}$.[2] This complex exhibits a long-lived metal to ligand charge transfer (MLCT) excited state (850 ns). It was later found to be capable of excited state energy and electron transfer.[3-6] Therefore, $[Ru(bpy)_3]^{+2}$ has potential applications in photochemical schemes.[7-8] $[Ru(bpy)_3]^{+2}$ is a relatively efficient excited state electron transfer agent, but is only capable of transferring one electron to a substrate. Back electron transfer also frequently limits the final quantum efficiency for electron transfer. Therefore $[Ru(bpy)_3]^{+2}$ analogs, which could potentially be covalently bound to other

units and are still capable of excited state energy and electron transfer, have been reviewed.[7-11]

A wide variety of $[Ru(bpy)_3]^{+2}$ analogs have been synthesized and characterized. Their most common application is in supramolecular complexes with $[Ru(bpy)_3]^{+2}$ and $[Ru(bpy)_2(BL)]^{+2}$ analogs (where BL = bridging ligand) as light absorbers in photochemical molecular devices.[10,11] Many $[Ru(bpy)_2(BL)]^{+2}$ complexes have been synthesized and investigated (Figure 1.2). These include systems with bidentate and tridentate bridging ligands. Highlighted below are ruthenium complexes with bidentate bridging ligands, as they are the types of ligands used in this investigation.

For polypyridyl analogs of $[Ru(bpy)_3]^{+2}$ of the type $[Ru(bpy)_2(BL)]^{+2}$, the electronic absorption spectra consist of intraligand $n \rightarrow \pi^*$ and $\pi \rightarrow \pi^*$ transitions in the ultraviolet region, and MLCT transitions in the visible (Table 1.1). For this discussion, the bridging ligands dpp, dpq, and dpb are considered (dpp = 2,3-bis(2-pyridyl)pyrazine, dpb = 2,3-bis(2-pyridyl)benzoquinoxaline, and dpq = 2,3-bis(2-pyridyl)quinoxaline). The lowest lying excited state is typically $Ru(d\pi) \rightarrow BL(\pi^*)$ charge transfer. The energy at which this lowest lying MLCT occurs varies as the bridging ligand is varied. In a series of bridging ligands commonly employed by the Brewer group, this MLCT transition is shifted to lower energy as the bridging ligand is changed from dpp to dpq to dpb. This is attributed to decreasing π^* orbital energies: dpp > dpq > dpb. Thus $Ru \rightarrow BL$ charge transfer excited states direct electron flow toward the position where another metal can be bound when constructing polymetallic systems.

Electrochemistry is commonly used to study transition metal polypyridyl complexes. For $[Ru(bpy)_2(BL)]^{+2}$, the highest-occupied molecular orbital (HOMO) is $Ru(d\pi)$ based and the lowest-unoccupied molecular orbital (LUMO) is typically $BL(\pi^*)$ based. For this type of mixed-ligand polyazine ruthenium complex, the electrochemistry is dominated by metal-based oxidations and ligand-based reductions. The ligand reduction is shifted to a lower potential with ligands that have lower-lying π^* orbitals.[3,10,12] This is illustrated in Table 1.1. The first reduction for the series of

$[Ru(bpy)_2(BL)]^{+2}$ complexes is assigned to the bridging ligand ($BL^{0/-}$). This reduction shifts as the bridging ligand is varied, with the dpb complex at the most positive potential, followed by dpq, then dpp (Table 1.2). As the redox and spectroscopic orbitals are the same it is possible, therefore, to tune the properties of the metal-to-ligand charge transfer (MLCT) by varying the bridging ligand.[15]

Figure 1.2. Selected Bidentate Polypyridyl Ligands.

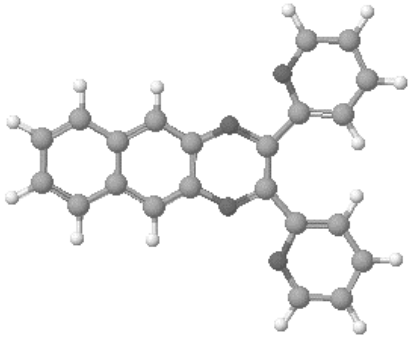

dpb

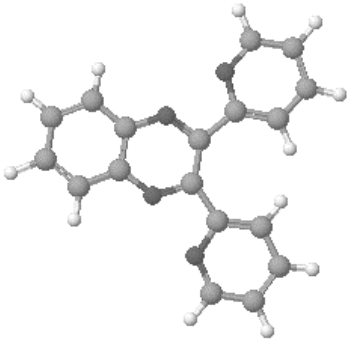

dpq

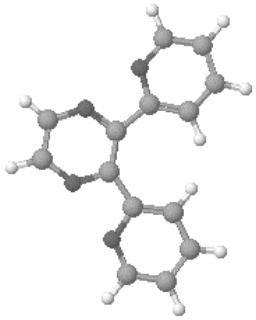

dpp

Where dpp = 2,3-bis(2-pyridyl)pyrazine, dpb = 2,3-bis(2-pyridyl)benzoquinoxaline, dpq = 2,3-bis(2-pyridyl)quinoxaline. Atom Types: black = nitrogen, gray = carbon, white = hydrogen.

Table 1.1. Electronic Absorption Spectral Data for a Series of Monometallic Ruthenium Polypyridyl Complexes of the form $[(bpy)_2Ru(BL)]^{+2}$, where dpp = 2,3-bis(2-pyridyl)pyrazine, dpq = 2,3-bis(2-pyridyl)quinoxaline, dpb = 2,3-bis(2-pyridyl)benzoquinoxaline, and bpy = 2,2'-bipyridine.[a]

Complex	Wavelength (nm)	Assignment
$[(bpy)_2Ru(dpp)]^{+2}$ [b]	286	bpy $\pi \rightarrow \pi^*$
	430	$Ru(d\pi) \rightarrow bpy(\pi^*)$ MLCT
	470 (sh)	$Ru(d\pi) \rightarrow dpp(\pi^*)$ MLCT
$[(bpy)_2Ru(dpq)]^{+2}$ [c]	284	bpy $\pi \rightarrow \pi^*$
	344 (sh)	dpq $\pi \rightarrow \pi^*$
	426	$Ru(d\pi) \rightarrow bpy(\pi^*)$ MLCT
	517	$Ru(d\pi) \rightarrow dpq(\pi^*)$ MLCT
$[(bpy)_2Ru(dpb)]^{+2}$ [d]	286	bpy $\pi \rightarrow \pi^*$
	362 (sh)	dpb $\pi \rightarrow \pi^*$
	394	$Ru(d\pi) \rightarrow bpy(\pi^*)$ MLCT
	550	$Ru(d\pi) \rightarrow dpb(\pi^*)$ MLCT

a. Spectra were recorded in acetonitrile.
b. references 13, 14
c. references 14, 15
d. reference 16

Table 1.2. Cyclic Voltammetric Data for a Series of Monometallic Ruthenium Polypyridyl Complexes of the form $[(bpy)_2Ru(BL)]^{+2}$, where dpp = 2,3-bis(2-pyridyl)pyrazine, dpq = 2,3-bis(2-pyridyl)quinoxaline, dpb = 2,3-bis(2-pyridyl)benzoquinoxaline, and bpy = 2,2'-bipyridine.

Complex	$E_{1/2}$ (V)	Assignment
$[(bpy)_2Ru(dpp)]^{+2}$ [a]	+1.41	$Ru^{II/III}$
	-1.02	$dpp^{0/-}$
	-1.45	$bpy^{0/-}$
	-1.67	$bpy^{0/-}$
$[(bpy)_2Ru(dpq)]^{+2}$ [b]	+1.40	$Ru^{II/III}$
	-0.79	$dpq^{0/-}$
	-1.40	$bpy^{0/-}$
	-1.65	$bpy^{0/-}$
$[(bpy)_2Ru(dpb)]^{+2}$ [c]	+1.40	$Ru^{II/III}$
	-0.64	$dpb^{0/-}$
	-1.28	$bpy^{0/-}$
	-1.63	$bpy^{0/-}$

Measurements taken in CH_3CN with 0.1 M Bu_4PF_6 supporting electrolyte, 200 mv/s scan rate. Potentials reported versus Ag/AgCl reference electrode (0.29 V vs. NHE, 0.44 V vs. $Cp_2Fe^{0/+1}$).

a. references 13, 14
b. references 14, 15
c. reference 16

Rhodium Polypyridyl Complexes.

Ru^{II} complexes have been used as photocatalysts. The isoelectronic d^6 Rh^{III} polypyridyl complexes, however, have been much less thoroughly investigated.[17] The preparation of Rh^{III} polypyridyl complexes was introduced in 1934 by F. Jaeger and J.

van Dijk.[17,18] The authors reported the synthesis and characterization of $[Rh(bpy)_3]Cl_3$ and $[Rh(bpy)_2Cl_2]Cl$, although both complexes were impure.[17] Martin et al.[19], and McKenzie et al.[20] reported the preparation of the same complexes, with characterization to establish their purity.

McKenzie and Plowman later reported that although in theory $[Rh(bpy)_2Cl_2]Cl$ may exist as a *cis*- or *trans*-geometric isomer, only the *cis*- octahedral configuration results.[17] This selectivity was attributed to α-hydrogen steric interaction between the two bpy moieties in the *trans*- octahedral configuration.[17] The *trans*-$[Rh(bpy)_2Cl_2]Cl$ configuration has since been reported.[21]

The lowest lying excited state of $[Rh(bpy)_3]^{+3}$ differs from that of $[Ru(bpy)_3]^{+2}$. The ruthenium complex's lowest lying excited state is $Ru(d\pi) \rightarrow bpy(\pi^*)$ CT based, whereas the lowest lying excited state of $[Rh(bpy)_3]^{+3}$ has been reported to be largely ligand based ($\pi \rightarrow \pi^*$).[22] The MLCT nature of the $[Ru(bpy)_3]^{+2}$ lowest lying excited state results in different properties than the $\pi \rightarrow \pi^*$ nature of the $[Rh(bpy)_3]^{+3}$ lowest lying excited state. Although $[Rh(bpy)_3]^{+3}$ and $[Ru(bpy)_3]^{+2}$ are isoelectronic and isostructural, $[Rh(bpy)_3]^{+3}$ is not a desirable excited state electron transfer agent.

There are also distinct differences in the electrochemistry of these two complexes, $[Rh(bpy)_3]^{+3}$ and $[Ru(bpy)_3]^{+2}$. The first reduction displayed in the CV of $[Rh(bpy)_3]^{+3}$ is ligand based and is followed by a rhodium based reduction, there are no oxidations present in the electrochemistry of this system.[22] The ruthenium analogue, however, has a ruthenium oxidation, and all reductions are ligand based.

Analogues of $[Rh(bpy)_2Cl_2]^+$ have been investigated by several researchers.[17,23,24] The electrochemistry of $[Rh(BL)_2Cl_2]^+$, where BL = dpp, dpq, and dpb, is summarized in Table 1.3. For $[Rh(BL)_2Cl_2]^{+1}$, the highest-occupied molecular orbital (HOMO) is $Rh(d\pi)$ based and the lowest-unoccupied molecular orbital (LUMO) is mainly $Rh(d\sigma^*)$.[24] Cyclic voltammetric data shows the first reduction to be at rhodium, followed by subsequent bridging ligand reductions. The bridging ligand reductions shift to more

positive potential as the ligand is varied, from dpp to dpq to dpb. This is attributed to decreasing π^* orbital energies in the order: dpp, dpq, dpb.

Table 1.3. Cyclic Voltammetric Data for a Series of Monometallic Rhodium Polypyridyl Complexes of the form $[Rh(BL)_2Cl_2]^{+1}$, and $[Rh(bpy)_2Cl_2]^{+1}$, where dpp = 2,3-bis(2-pyridyl)pyrazine, dpq = 2,3-bis(2-pyridyl)quinoxaline, dpb = 2,3-bis(2-pyridyl)benzoquinoxaline, and bpy = 2,2'-bipyridine.

Complex	$E_{1/2}$ (V)	Assignment
$[Rh(bpy)_2Cl_2]^{+1}$ [a]	-0.80	$Rh^{III/I}$
	-1.30	$bpy^{0/-}$
	-1.50	$bpy^{0/-}$
$[Rh(dpp)_2Cl_2]^{+1}$ [b]	-0.60	$Rh^{III/I}$
	-1.05	$dpp^{0/-}$
	-1.19	$dpp^{0/-}$
$[Rh(dpq)_2Cl_2]^{+1}$ [b]	-0.44	$Rh^{III/I}$
	-0.85	$dpq^{0/-}$
	-1.49	$dpq^{0/-}$
$[Rh(dpb)_2Cl_2]^{+1}$ [b]	-0.39	$Rh^{III/I}$
	-0.72	$dpb^{0/-}$
	-1.24	$dpb^{0/-}$

Measurements taken in CH_3CN with 0.1 M Bu_4PF_6 supporting electrolyte, 200 mv/s scan rate. Potentials reported versus Ag/AgCl reference electrode (0.29 V vs. NHE, 0.44 V vs. $Cp_2Fe^{0/+1}$).

a. Reference 24.
b. Reference 25.

DeArmond and co-workers examined the electrochemical properties of several Rh^{III} polypyridyl/N-N complexes, where N-N is a bidentate nitrogen donor ligand.[5,25-32] A cyclic voltammetric study of $[Rh(bpy)_2Cl_2]^+$ showed the first reduction to be at rhodium, followed by subsequent reductions of the bpy ligands.[25] The rhodium reduction

results from two subsequent one-electron reductions of the Rh^{III} center and is irreversible. The first one-electron transfer was followed by chemical reaction – loss of chloride, as detected by an irreversible wave ca. + 1.4 V.[25] An ECEC (electrochemical-chemical-electrochemical-chemical) mechanism was proposed for the reduction of $[Rh(bpy)_2Cl_2]^+$ (Scheme 1.1).

Scheme 1.1. Proposed ECEC Mechanism for the Two-Electron Reduction of $[Rh(bpy)_2Cl_2]^+$ by Cyclic Voltammetry, where ECEC = electrochemical-chemical-electrochemical-chemical, S = solvent, and bpy = 2,2'-bipyridine.[25]

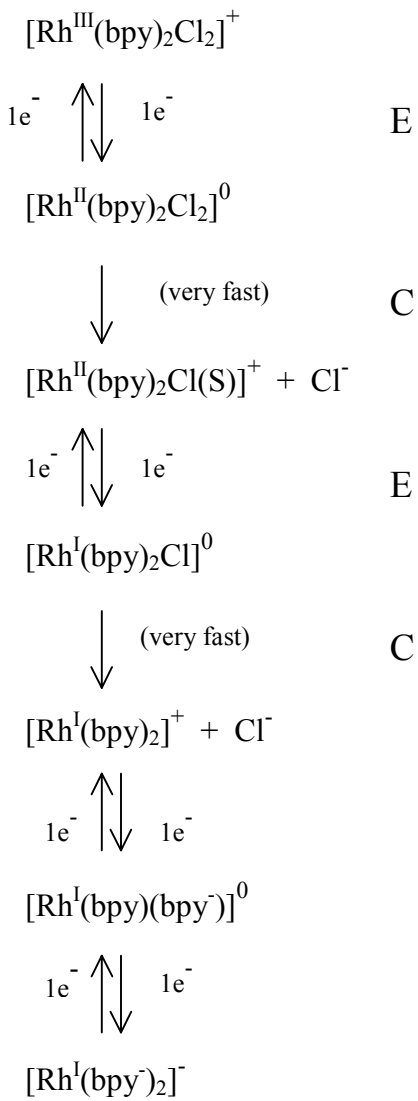

The two-electron reduction of $[Rh(bpy)_2Cl_2]^+$ results in the conversion of the rhodium from d^6 to d^8. In the initial complex $[Rh(bpy)_2Cl_2]^+$, the d^6 rhodium is pseudo-octahedral. Upon conversion from the Rh^{III} d^6 electron configuration to Rh^I d^8, the stable rhodium geometry becomes square planar. This results in the loss of two ligands, two chlorides, via a chemical step. Therefore, the two-electron reduction product of $[Rh(bpy)_2Cl_2]^+$ is the square planar Rh^I complex, $[Rh(bpy)_2]^+$.[25]

As seen in Scheme 1.1, after the Rh^{III} center is reduced by one electron, a rapid chemical step occurs. The subsequent rhodium reduction ($Rh^{II/I}$) is also followed by a rapid loss of one chloride ligand, which results in $[Rh(bpy)_2]^+$. These steps encompass the ECEC portion of the electrochemical mechanism. DeArmond and others have successfully studied ECE(C) electrochemical mechanisms with related complexes, including $[Rh(bpy)_3]^{+3}$ [25] and $[Rh(1,10\text{-phen})_3]^{+3}$,[26] wherein a chelate is lost, and $[Rh(1,10\text{-phen})_2Cl_2]^+$.[27]

Watts[33-34], Morrison[35], DeArmond[5,36], Crosby[37], and Barton[38-41] have investigated mixed-ligand complexes incorporating N-N bidentate ligands. Watts investigated the energy gaps between the ground state and $^3\pi \rightarrow \pi^*$ for $[Rh(bpy)_n(phen)_{3-n}]Cl_3$ and substituted 1,10-phenanthroline complexes via emission spectroscopy. Crosby studied the excited states of a related 1,10-phenanthroline complex, $[Rh(bpy)_m(phen)_n]Cl_3$, where m= 3-n, and n= 0,1,2,3.[37] The authors found that for this series of complexes the lowest excited state is $^3\pi \rightarrow \pi^*$, and that there is very little interligand interaction in both the ground and lowest excited state.

Rh^{III} polypyridyl complexes have potential applications in catalysis. Monometallic Rh^{III} polypyridyl complexes electrocatalyze the reduction of CO_2 to carbon monoxide and formate (major products).[42-44] Multimetallic Rh^{III} polypyridyl complexes electrocatalyze the reduction of CO_2 to methanol and methane.[43-46] Multimetallic Rh^{III} polypyridyl complexes are required to electrocatalyze the above

reactions due to the large number to electrons needed for the desired CO_2 reduction.[24] Rh^{III} polypyridyl complexes can also used as a catalyst precursor for the water gas shift (WGS) reaction (Equation 1).

$$H_2O + CO \longleftrightarrow H_2 + CO_2 \qquad (1)$$

Creutz and co-workers found $Rh(bpy)_2^+$ in the presence of triethanolamine to be an effective catalyst precursor for homogeneous catalysis of the water gas shift reaction under mild conditions (<100 °C and <1 atm CO).[47-49] The combination of $Rh(bpy)_2^+$ with $Ru(bpy)_3^{+2}$ (in the presence of triethanolamine) has also been found to be a successful component in the photoreduction of H_2O to H_2 by Creutz and Sauvage.[50-51] Additionally, Mulazzani and Hoffman have found the reaction of $Rh(bpy)_3^{+3}$ with reducing radicals in aqueous solution capable of reducing H_2O to H_2 in the absence of a catalyst.[52]

Photochemical Molecular Devices for Photoinitiated Electron Collection.

A photochemical molecular device is a supramolecular complex comprised of several different subunits. Each subunit has it own purpose, in the function of the molecular device. The action of each subunit, when performed in a particular sequence, yields the overall function of the device. Each subunit in the supramolecular complex maintains its basic properties. This is essential to the development of photochemical molecular devices, because each subunit was chosen to perform a job based on its properties.

Balzani proposed a theory describing the orbital diagrams for several photochemical molecular devices (PMD).[53] One of these is the device for photoinitiated electron collection (PEC). The molecular device for PEC is comprised for three types of subunits: light absorber (LA), electron donor (ED), and electron collector (EC). Our representation of the orbital properties of his proposed device is shown in Figure 1.3. The subunits are covalently bound to each other, and can be organic or inorganic in nature. Each selected subunit should maintain its basic properties when brought into the

assembly. The goal of this molecular device is light initiated collection at multiple electrons on a central reservoir (electron collector).

PEC is accomplished in a series of steps. In the presence of light (hν), an electron on the LA portion of the molecule is promoted to an acceptor orbital. This leaves a hole in the donor orbital of the light absorber, which, if not filled, will allow the promoted electron to fall back to the donor orbital. Electron donors are used to prevent this. The electron in the initial acceptor orbital will then be transferred to the lower energy orbital localized on the electron collector. This process is repeated on the other half of the molecule. The net result of photoinitiated electron collection is a two-electron reduced EC, and two ED moieties, which are oxidized by one electron each (Figure 1.3).

First Device for Photoinitiated Electron Collection.

The first device for photoinitiated electron collection was developed by Brewer.[54-56] This supramolecular device, $\{[(bpy)_2Ru(dpb)]_2IrCl_2\}(PF_6)_5$, is capable of photoinitiated electron collection in the presence of a sacrificial electron donor (ED), dimethylaniline.[55] Two electrons are collected on the EC portion of the molecule, $(dpb)Ir^{III}Cl_2(dpb)$, resulting in $\{[(bpy)_2Ru(dpb^-)]_2IrCl_2\}(PF_6)_3$. The orbital energy diagram for this device is presented in Figure 1.4. In the presence of light (hν), the light absorber (Ru) subunit produces an MLCT excited state, which is quenched by the electron donor. This process is repeated with the other light absorber subunit, to result in two-electron collection on the electron collector. Dimethylaniline is used as a sacrificial electron donor (quencher), to prevent back electron transfer. The orbital energy diagram for $\{[(bpy)_2Ru(dpb)]_2IrCl_2\}(PF_6)_5$ shows that the relative energy level of the $Ir(d\sigma^*)$ orbitals are higher than that of the bridging $dpb(\pi^*)$ orbitals. As a result the $(dpb)Ir^{III}(dpb)$ portion of the molecule acts as the electron collector, rather than the central metal alone.

Figure 1.3. Orbital Energy Diagram and Device Function for a Photochemical Molecular Device for Photoinitiated Electron Collection.

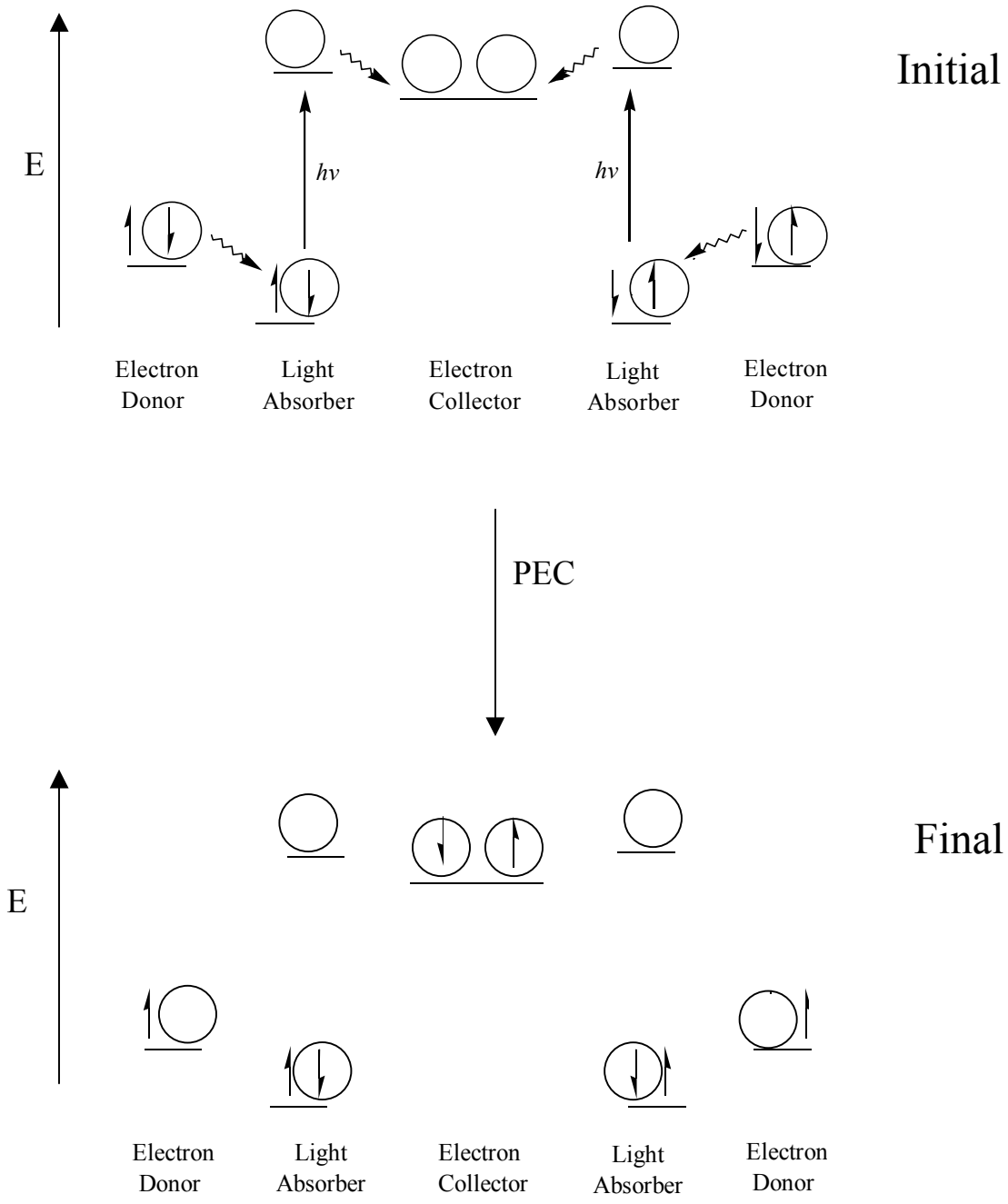

Figure 1.4. Orbital Energy Diagram for $\{[(bpy)_2Ru(dpb)]_2IrCl_2\}(PF_6)_5$.

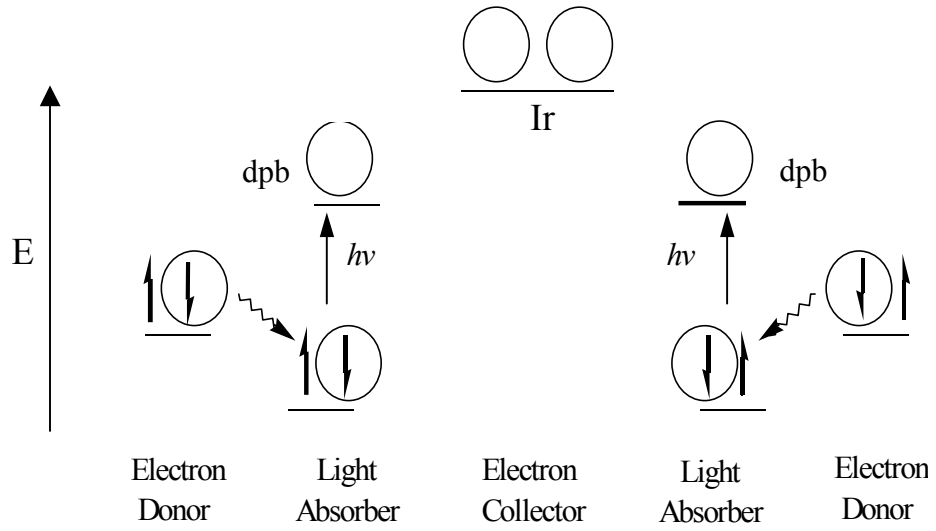

The net result of photoinitiated electron collection is a two-electron reduced (dpb)$IrCl_2$(dpb) core, and two one-electron oxidized dimethylaniline ED molecules. Upon reduction, the collected electrons are available for use by a substrate. The quantum yield for the production of the reduced species, however, is low. This is due in part to the fact that the molecular device has an estimated excited state lifetime of 4.5 ns, during which it must react with the electron donor.[55]

Mixed-Metal Polypyridyl Complexes of Rhodium(III).

A wide variety of both mono- and polymetallic transition metal polypyridyl systems have been synthesized and characterized. The scope of this research is broad; several recent reviews have been published.[8-11] These complexes are under investigation for potential photochemical and electrochemical applications.

Since the relative d orbital energy level of d^6 rhodium is lower than that of iridium, rhodium is more easily reduced. Therefore, it is potentially effective as the electron collection part of a supramolecular device. In the mixed metal complexes $[(tpy)Ru(tpy\text{-}(Ph)_n\text{-}tpy)Rh(tpy)]^{+5}$, where (n = 0, 1, 2) and tpy is 2,2',6',2''-terpyridine,

electron transfer quenching of the Ru based MLCT excited state by the Rh^{III} center is observed at 150 K for the n = 0 complex, but not for the systems where n = 1 or 2.[57,66] The difference is attributed to the increase in distance between the donor and the acceptor created by the phenylene spacers.[66] Therefore, $[(tpy)Ru(tpy\text{-}tpy)Rh(tpy)]^{+5}$ represents a light-absorber – electron acceptor dyad.[66] It should be noted that with tris-chelate complexes, no following chemical reaction is observed after electron transfer. The complex $[Ru(Me_2phen)_2\text{-}(Mebpy\text{-}CH_2CH_2\text{-}Mebpy)Rh(Me_2bpy)_2]^{+5}$, where Mebpy = 4-methyl-2,2'-bipyridine, Me_2bpy = 4,4'-dimethyl-2,2'-bipyridine, Me_2phen = 4,7-dimethyl-1,10-phenanthroline, undergoes electron-transfer quenching of the Ru-based MLCT excited state by the Rh center.[58,59,66]

The monometallic complex $[Rh(dpp)_2Cl_2]^+$ shows a metal-centered (d $\rightarrow$ d) lowest excited state[60], where $[Rh(bpy)_2(dpp)]^{+3}$, and $[Rh(dpp)_2(bpy)]^{+3}$ exhibit strong ligand-centered ($\pi \rightarrow \pi^*$) lowest excited states.[62] Using the above systems as "parent complexes" leads to rational trends in the excited-state properties of mixed-metal Rh^{III} polypyridyl complexes, such as $[(bpy)_2Ru(dpp)Rh(bpy)_2]^{+5}$, a chromophore-quencher complex.[43, 63-65] This proposed photophysical pathway differs from the others presented, as it proposes a MMCT (metal to metal charge transfer) rather than MLCT excitation (Equations 2-4[60-61]).

$$[(bpy)_2Ru^{II}(dpp)Rh^{III}(bpy)_2]^{+5} \xrightarrow{h\nu} {}^*[(bpy)_2Ru^{III}(dpp)Rh^{II}(bpy)_2]^{+5} \quad (2)$$

$${}^*[(bpy)_2Ru^{III}(dpp)Rh^{II}(bpy)_2]^{+5} \xrightarrow{ET} [(bpy)_2Ru^{III}(dpp^-)Rh^{III}(bpy)_2]^{+5} \quad (3)$$

$$[(bpy)_2Ru^{III}(dpp^-)Rh^{III}(bpy)_2]^{+5} \xrightarrow{ET} [(bpy)_2Ru^{II}(dpp)Rh^{III}(bpy)_2]^{+5} \quad (4)$$

Brewer and co-workers have studied a variety of Rh^{III} complexes as light absorber – electron acceptor dyads and in the development of supramolecular devices for photoinitiated electron collection.[23,55,66-67] Light absorber – electron acceptor dyads

couple a Ru^{II} polypyridyl subunit as a light absorber with a Rh^{III} electron acceptor. The use of the tridentate bridging ligand 2,3,5,6-tetrakis(2-pyridyl)pyrazine (tpp) in the bimetallic complex $[(tpy)Ru(tpp)RhCl_3]^{+2}$ provides a stereochemically defined light absorber – electron acceptor dyad (tpy = 2,2',6,2''-terpyridine).[66] Cyclic voltammetry showed the first reduction to be $Rh^{III/I}$ based (-0.23 V), followed by subsequent bridging reductions.[66] Thus, the LUMO for $[(tpy)Ru(tpp)RhCl_3]^{+2}$ is rhodium-based. The lowest-lying electronic transition was determined to be a Ru → tpp charge transfer. Following excitation of the complex into the Ru → tpp charge-transfer state, electron transfer to the Rh^{III} LUMO is observed.[66]

Complexes of the type $\{[(bpy)_2Ru(BL)]_2RhCl_2\}^{+5}$, where BL = dpp, dpq, dpb, or bpm, have also been investigated; investigation of the dpp, dpq, and dpb series was preliminary work.[55] The complex $\{[(bpy)_2Ru^{II}(dpp)]_2Rh^{III}Cl_2\}^{+5}$ is the subject of this thesis. This complex was synthesized by coupling two $[Ru^{II}(bpy)_2(dpp)]^{+2}$ units to a central $RhCl_3$ core.[55] Purification was achieved by size exclusion chromatography. Cyclic voltammetric data for this complex is presented in Table 1.4, with the cyclic voltammetric data for the Ir^{III} and Ru^{II} analogs presented for comparison. The HOMO of $\{[(bpy)_2Ru(bpm)]_2RhCl_2\}^{+5}$ is ruthenium-based, while the LUMO is bpm-based. This bpm-based LUMO is in contrast to the rhodium based LUMO observed $[Rh(bpm)_2Cl_2]^{+}$. The observed orbital inversion is attributed to bpm bridge formation in construction of the trimetallic complex, leading to a stabilization of the bpm π^* orbitals and bringing them below the Rh($d\sigma^*$) set.[67]

The Rh^{III}, Ir^{III}, and Ru^{II} analogs of $\{[(bpy)_2Ru(dpp)]_2MCl_2\}^{n+}$ exhibit different electrochemical properties.[55,68] For the rhodium complex, the first reduction $Rh^{III/I}$, indicating that the LUMO is rhodium-based. The iridium complex $\{[(bpy)_2Ru(dpp)]_2IrCl_2\}^{+4}$ also has a dpp-based LUMO as μ-dpp that is reduced much more easily than the central iridium.[55] The ruthenium trimetallic complex $\{[(bpy)_2Ru(dpp)]_2RuCl_2\}^{+n}$ shows two reversible $Ru^{II/III}$ oxidations, as there are two

different ruthenium environments.[68] This complex has a dpp-based LUMO. All three complexes exhibit ruthenium-based HOMOs. These preliminary electrochemical properties suggest that the rhodium complex $\{[(bpy)_2Ru(dpp)]_2RhCl_2\}^{+5}$ is best suited for electron collection on the central metal. The goal of this thesis is to evaluate this hypothesis.

Table 1.4. Cyclic Voltammetric Data for $\{[(bpy)_2Ru(dpp)]_2RhCl_2\}(PF_6)_5$, $\{[(bpy)_2Ru(dpp)]_2RuCl_2\}(PF_6)_4$, and $\{[(bpy)_2Ru(dpp)]_2IrCl_2\}(PF_6)_5$, where dpp = (2,3-bis(2-pyridyl)pyrazine), and bpy = 2,2'-bipyridine.

Complex	$E_{1/2}$ (V)	Assignment
$\{[(bpy)_2Ru(dpp)]_2RhCl_2\}^{+5}$ [a]	+1.56	$2Ru^{II/III}$
	-0.35	$Rh^{III/I}$
	-0.74	$dpp^{0/-}$
$\{[(bpy)_2Ru(dpp)]_2\mathbf{Ru}Cl_2\}^{+4}$ [b]	+0.83	$\mathbf{Ru}^{II/III}$
	+1.60	$2Ru^{II/III}$
	-0.71	$dpp^{0/-}$
	-0.88	$dpp^{0/-}$
	-1.43	$dpp^{-/-2}$
	-1.52	$dpp^{-/-2}$
$\{[(bpy)_2Ru(dpp)]_2IrCl_2\}^{+5}$ [a]	+1.56	$Ru^{II/III}$
	-0.39	$dpp^{0/-}$
	-0.54	$dpp^{0/-}$
	-1.06	$dpp^{-/-2}$
	-1.22	$dpp^{-/-2}$

Measurements taken in CH_3CN with 0.1 M Bu_4PF_6 supporting electrolyte, 200 mv/s scan rate. Potentials reported versus Ag/AgCl reference electrode (0.29 V vs. NHE, 0.44 V vs. $Cp_2Fe^{0/+1}$).

a. reference 55
b. reference 68